Mercury photolytic transformation affected by low-molecular-weight natural organics in water

4 AUTHORS:

Feng he
Zhejiang University of Technology
27 PUBLICATIONS   1,570 CITATIONS

SEE PROFILE

Wang Zheng
University of Toronto
13 PUBLICATIONS   539 CITATIONS

SEE PROFILE

Liyuan Liang
Oak Ridge National Laboratory
148 PUBLICATIONS   4,747 CITATIONS

SEE PROFILE

Baohua Gu
Oak Ridge National Laboratory
160 PUBLICATIONS   6,671 CITATIONS

SEE PROFILE

Mercury photolytic transformation affected by low-molecular-weight natural organics in water

Feng He *, Wang Zheng, Liyuan Liang, Baohua Gu **

Environmental Science Division, Oak Ridge National Laboratory Oak Ridge, Tennessee, 37831, United States

ABSTRACT

Mechanisms by which dissolved organic matter (DOM) mediates the photochemical reduction of Hg(II) in aquatic ecosystems are not fully understood, owing to the heterogeneous nature and complex structural properties of DOM. In this work, naturally occurring aromatic compounds including salicylic, 4-hydrobenzoic, anthranilic, 4-aminobenzoic, and phthalic acid were systematically studied as surrogates for DOM in order to gain an improved mechanistic understanding of these compounds in the photoreduction of Hg(II) in water. We show that the photoreduction rates of Hg(II) are influenced not only by the substituent functional groups such as –OH, –NH$_2$ and –COOH on the benzene ring, but also the positioning of these functional groups on the ring structure. The Hg(II) photoreduction rate decreases in the order anthranilic acid > salicylic acid > phthalic acid according to the presence of the –NH$_2$, –OH, –COOH functional groups on benzoic acid. The substitution position of the functional groups affects reduction rates in the order anthranilic acid > 4-aminobenzoic acid and salicylic acid > 4-hydroxybenzoic acid. Reduction rates correlate strongly with ultraviolet (UV) absorption of these compounds and their concentrations, suggesting that the formation of organic free radicals during photolysis of these compounds is responsible for Hg(II) photoreduction. These results provide insight into the role of low-molecular-weight organic compounds and possibly DOM in Hg photoredox transformation and may thus have important implications for understanding Hg geochemical cycling in the environment.

© 2011 Elsevier B.V. All rights reserved.

1. Introduction

Natural organics-mediated reduction and oxidation of mercury (Hg) both in dark and light (Amyot et al., 1994, 1997a; Gu et al., 2011; Krabbenhoft et al., 1998; Poulain et al., 2004; Ravichandran, 2004; Xiao et al., 1995; Zhang, 2006; Zhang and Lindberg, 2001; Zheng et al., in press) are known to critically influencing Hg geochemical cycling, species transformation and bioavailability. In surface water, photochemically induced Hg redox reactions are particularly important although detailed mechanisms are not well understood. Mercuric Hg(II) species can be reduced by solar radiation in the presence of naturally dissolved organic matter (DOM), producing dissolved gaseous mercury (DGM) in natural environments (Amyot et al., 1997b; O'Driscoll et al., 2003). However, depending on its origin, DOM differs in chemical composition and structural properties, which may reflect mixed results on its role in Hg photoreduction processes. For example, Amyot et al. (1997b) observed higher DGM production in a low-DOM lake with 2.2 mg L^{-1} dissolved organic carbon (DOC) than in two high-DOM lakes (5–8.7 mg L^{-1} DOC). On the other hand, O'Driscoll et al. (2003) reported that DOM production rates were higher in a high-DOM lake

(10.5 mg L^{-1} DOC) than in a low-DOM lake (3.6 mg L^{-1} DOC) in southern Nova Scotia, Canada, and a positive correlation was found between DGM production and DOC concentration (O'Driscoll et al., 2004). However, without detailed characterization of these DOM materials, it is difficult to generalize if these observed differences were a result of the amount of DOM present or the chemical and structural properties of DOM.

Low-molecular-weight organic compounds (LMWOCs, MW < ~1000), particularly aromatics (Benner et al., 1992), are the building blocks of DOM and can serve as good surrogates for DOM with varying structural and functional properties for studies of interactions between Hg and DOM (Zheng and Hintelmann, 2010). A significant advantage of using these organics is that their chemical structures and binding constants with Hg(II) are known (Haitzer et al., 2002; Ravichandran, 2004). In addition, these LMWOCs are produced by photodegradation of DOM in natural waters (Brinkmann et al., 2003; Moran and Zepp, 1997; Zhou and Mopper, 1997) and can contribute significantly to Hg(II) photoreduction in situ (Ababneh et al., 2006; Si and Ariya, 2008). As a soft Lewis acid, Hg(II) binds principally to reactive thiol (–SH) functional groups in DOM. However, Hg(II) also binds to carboxyls (–COOH) and hydroxyls (–OH) at high Hg(II)/DOM ratios (Haitzer et al., 2002; Dong et al., 2011). Zheng and Hintelmann (2010) recently evaluated the effect of LMWOCs on the photoreactivity and isotope fractionation of Hg and observed that thiols versus non-thiol LMWOCs can induce different mass-independent isotope effects during Hg(II)

---

* Corresponding author. Tel.: +1 865 574 5278; fax: +1 865 576 8646.
** Corresponding author. Tel.: +1 865 574 7286; fax: +1 865 576 8543.
  E-mail addresses: hef2@ornl.gov (F. He), gub1@ornl.gov (B. Gu).

photoreduction. This isotope effect also suggests that thiol- and non-thiol LMWOCs invoke different photochemical reduction mechanisms although systematic understanding of these organics on Hg(II) photo-reduction is yet to be determined.

In this study, we describe the photoreduction of Hg(II) (as HgCl$_2$) in the presence of selected non-thiolate aromatic compounds including salicylic, 4-hydrobenzoic, anthranilic, 4-aminobenzoic, and phthalic acids under controlled environmental conditions (e.g., pH, Cl$^-$ concentration, irradiation wavelength and intensity). These LMWOCs vary in substituent functional groups (i.e., –OH, –NH$_2$ and –COOH) and their positioning on the benzene ring structure. They were chosen to represent an important class of dissolved organics that are commonly observed in natural waters (Brinkmann et al., 2003; Moran and Zepp, 1997; Zheng and Hintelmann, 2010; Zhou and Mopper, 1997) and thus may influence on Hg photoredox transformation and cycling in the environment. The Hg(II) photoreduction rates were determined and compared at the same equivalents of substituent functional groups of either –OH, –NH$_2$, or –COOH in solution.
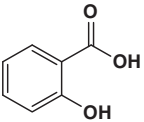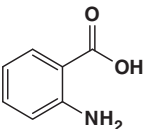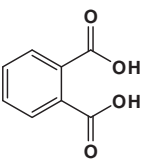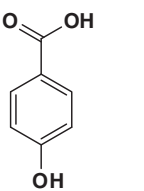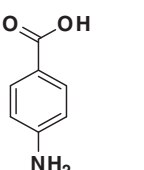
2. Materials and methods

All chemicals used in the experiments were either ACS reagent grade or better, and their selected physicochemical properties are listed in Table 1. Hg(II) stock solutions (20 nM in 0.12 M HCl) were prepared from a reference standard (1000 µg/mL in 3% HNO$_3$, Ricca Chemical Company). The photoreduction experiments were conducted using a LuzChem ICH-2 photoreactor equipped with 6 lamps of either UV-B (280–320 nm) or UV-A (320–400 nm) light at the top of the reactor chamber (lamp spectra provided in the

Supplementary Data, Fig. S1). The UV-B lamps have 61.6%, 24.5%, 3.1%, and 10.2% of irradiation in UVB, UVA, UVC, and visible region, respectively. The UV-A lamps have 95.5%, 2.2%, 0.7%, and 1.3% in UVB, UVA, UVC, and visible region, respectively. Specific UVB and UVA spectra rather than simulated sunlight were used to establish correlation between individual radiation energy and the absorption characteristics of the organic compounds because, depending on the molecular structure, absorption of a given energy accounts for the formation of organic radicals (O'Driscoll et al., 2006; Qureshi et al., 2010). We note that, although the percentage of UV-B in sunlight is relatively low (up to 5% of UV), its contribution to Hg(II) photoreduction is significant (>23%) (Amyot et al., 1997a; Bonzongo and Donkor, 2003). In this study, the radiant fluxes received by the reactant solution were estimated to be ~31.0 W m^{-2} (with UVB 19.1 W m^{-2} and UVA 7.6 W m^{-2}) under UVB and ~33.6 W m^{-2} (with UVA 32.1 W m^{-2}) under UV-A irradiation. These UV values correspond to approximately 156% and 188% of full sun UVA intensity (~17.1 W m^{-2}) in the mid-summer in Eastern Tennessee (Zhang and Dill, 2008). The estimation of the irradiation energy is based on the lamp spectra and the measurement of photon flux using chemical actinometry (see Supplementary Data).

The reaction temperature was controlled at 23 ± 1 °C by an internal exhaust fan. High-purity N$_2$ was used to continuously purge DGM out of the reaction vessel during the photoreduction experiment. The use of N$_2$ was necessary to avoid photo-oxidation of both Hg(0) and LMWOCs by O$_2$, which interferes with the photoreduction process (Si and Ariya, 2008; Zheng and Hintelmann, 2009). DGM was analyzed directly by a Tekran 2537A analyzer in real-time with values logged every 2.5 min on a computer. The mass flow controller of Tekran

Table 1
Low-molecular-weight organic compounds (LMWOCs), chemical structures, pK$_a$ values, UV absorption peaks, concentrations, and pseudo-first-order photoreduction rates of Hg(II). Experiments were performed at 23 ± 1 °C, pH 4.2 ± 0.3, 1 nM HgCl$_2$, and 60 µM Cl$^-$. Estimated experimental errors between duplicate measurements were generally lower than ± 10%.

LMWOCs	Structure	pK$_a$[a]	UV absorption peak (nm)	Conc. (µM)	k_r (UV-B) (h^{-1})	k_r (UV-A) (h^{-1})
Blank	–		–	0	1.6 ± 0.3	0.31
Salicylic acid		3.00 (–COOH), 13.4 (–OH)	296	2	8.3 ± 0.1	0.60
				1	2.9	–
				0.2	2.1	–
Anthranilic acid		2.11 (–NH$_3^+$), 4.95 (–COOH)	313	2	8.8 ± 0.5	8.4
				0.2	5.6	–
				0.005	2.0	–
Phthalic acid		2.89, 5.51	280	2	3.4	–
4-Hydroxybenzoic acid		4.48 (–COOH), 9.32 (–OH)	250	2	2.4	0.33
4-Aminobenzoic acid		2.5 (–NH$_3^+$), 4.87 (–COOH)	271	2	7.6	1.8

[a] Data from Sillen et al., 1964.

2537A was calibrated to normal air mass, which shows negligible differences (<0.15%) when pure N$_2$ gas is used. The detection limit was <0.1 ng m^{-3} in a 7.5 L gas sample. High-purity argon and air were used as the carrier gas and zero-mercury gas, respectively, for the operation of the analyzer. Additional details of the experimental setup can be found in Fig. S2, Supplementary Data, in which a T-valve was used to release excess N$_2$ and thus to balance the N$_2$ flow into the reactor (Qureshi et al., 2010).

A quartz flask (8.4×15 cm, QSI Scientific) with a silicon stopper was used for the photoreduction experiments. The reactor was first cleaned with BrCl solution and thoroughly rinsed with deionized (DI) water before initiating the experiments. A glass sparger was fitted through the center of the silicon stopper to carry N$_2$ into the reactant solution.

We followed DGM production as a measure of Hg(II) reduction under controlled experimental conditions. In a typical experiment, 200 mL of DI water was first added to the reactor, followed by addition of stock Hg and LMWOC solutions. The initial Hg concentration was ~1 nM and the LMWOC concentration ranged from 5 nM to 2 μM. For most of the experiments, the pH of the reaction solution was maintained at 4.2±0.3 and Cl$^-$ concentration at 60 μM so that Hg(II) was in the dominant form of HgCl$_2$ in solution (Dong et al., 2010) for the photoreduction experiment. This ensures that similar Hg(II) species were present in the reactant solution for comparison of the reaction rates. For selected experiments, a pH of 8.0±0.1 was used to evaluate the effect of pH on Hg(II) photoreduction. Before irradiation, the reactant solution was purged with N$_2$ for at least 20 min in the dark to remove any DGM (monitored by Tekran 2537A) and dissolved oxygen. Therefore, the DGM readings following UV irradiation were the result of the photoreduction. The reactant solution was irradiated until negligible DGM was measured from the Tekran analyzer. Samples before and after the photoreduction were also collected and analyzed to determine the total Hg concentrations so that a mass balance could be determined. These samples were oxidized in 1% BrCl overnight, and the total Hg was analyzed using an automated cold vapor atomic fluorescence spectrometry (CVAFS) system (Tekran 2600). Dark control experiments were performed similarly. The fraction of Hg lost in the process is attributed to the adsorption of Hg on the reactor wall or the sparger. This fraction was generally less than 10% of Hg(II) in our experiments. Estimated errors from duplicate experiments were within ±10%.

The pseudo-first-order reaction kinetics was found to fit experimental data at the initial stage of the reaction. The rate constant was calculated as follows (Qureshi et al., 2010):

$$d([Hg(II)]_r/[Hg]_T)/dt = -k_r([Hg(II)]_r/[Hg]_T) \quad (1)$$

$$d([DGM]/[Hg]_T)/dt = k_r([Hg(II)]_r/[Hg]_T) \quad (2)$$

where k_r is the rate constant for Hg(II) reduction, [Hg]$_T$ is the total Hg concentration, [Hg(II)]$_r$ is the Hg concentration in solution, and [DGM] is the mass of gaseous Hg(0) normalized by the volume of the reactant solution. If we neglect the loss of Hg due to sorption, [Hg(II)]$_r$/[Hg]$_T$ plus [DGM]/[Hg]$_T$ should be equal to 1. Then, Eq. (2) can be rewritten as:

$$\ln(1-[DGM]/[Hg]_T) = -k_r t \quad (3)$$

3. Results and discussion

3.1. LMWOC functional groups and steric arrangements on Hg(II) photoreduction

Effects of LMWOCs including anthranilic acid, salicylic acid, and phthalic acid on Hg(II) photoreduction rates were first determined under UV-B irradiation (Fig. 1a). These organic compounds have the same structural configuration as a benzoic acid, except that each compound is substituted at the ortho position with a different functional group (i.e., –NH$_2$, –OH, or –COOH) (Table 1). The presence of these LMWOCs increased the rate of Hg(II) photoreduction when compared with those without organics added (or HgCl$_2$ only) under the same experimental conditions. Importantly, the substitution of these functional groups resulted in substantial differences in the rates of Hg(II) photoreduction, which decreased in the order anthranilic acid (–NH$_2$)>salicylic acid (–OH)>phthalic acid (–COOH). This trend was even better represented when the organic concentration is decreased (Table 1). The reduction of Hg(II) can be well described by pseudo-first-order kinetics (Eq. (3)), with an observed correlation coefficient R>0.99 for data collected at [DGM]/[Hg]$_T$<~70%. At an organic concentration of 2 μM, the observed rates are 8.8, 8.3, and 3.4 h^{-1} in the presence of anthranilic acid, salicylic acid, and phthalic acid, respectively (Table 1). These rates are roughly 2–6 times higher than that in the absence of organic compounds (HgCl$_2$ only). Since only negligible amounts of Hg(II) (<2%) were reduced in the dark in the presence of either salicylic acid or anthranilic acid (Fig. 1a), this increased DGM production by LMWOC is attributed to the light-enhanced reduction of Hg(II).

We further examined the photoreduction rates of Hg(II) in the presence of two isomers of anthranilic acid and salicylic acid under the same experimental conditions (Fig. 1b). The substitution of the –NH$_2$ and –OH functional groups at the para-position, rather than the ortho-position, decreased the photoreduction rates. The first-order rate constants decreased from about 8.8 h^{-1} (anthranilic acid) to 7.6 h^{-1} (4-aminobenzoic acid), and from 8.3 h^{-1} (salicylic acid) to 2.4 h^{-1} (4-hydroxybenzoic acid), respectively (Table 1). These results clearly indicate that these LMWOCs are not merely providing a reductant in Hg(II) reduction; substitution of the –NH$_2$ or –OH functional groups at the ortho position of benzoic acid is most effective in enhancing the photoreduction of Hg(II) under UV-B irradiation.

The effects of LMWOC on Hg(II) photoreduction were also found to depend on the amount of organics in solution (Fig. 1c and d and Table 1). At the constant Hg(II) concentration of 1 nM, decreasing the salicylic acid from 2 to 0.2 μM led to a decrease of k_r from 8.3 to 2.1 h^{-1}. Similarly, decreasing the anthranilic acid from 2 to 0.2 μM led to a decrease of k_r from 8.8 to 5.6 h^{-1}, and to 2 h^{-1} when the acid was further decreased to 5 nM. This organic concentration-dependent photoreduction of Hg(II) suggests that the photolysis of LMWOCs produces photoreductants, which then attack Hg(II) to produce Hg(0). The higher the LMWOC concentrations, the more photoreductants are produced, leading to higher Hg(II) photoreduction rates. Such a reaction is often referred to as a secondary or indirect photolysis (Turro, 1978; Zhang, 2006), as opposed to direct photolysis of Hg-organic ligand complexes (Zhang, 2006; Zheng and Hintelmann, 2009, 2010). Direct photolysis involves ligand-to-metal charge transfer and is independent of ligand concentration. This charge transfer mechanism is referred to as the primary reaction and has been proposed as one of the dominant mechanisms for Hg(II) photochemical reduction in the presence of DOM (Zhang, 2006). This primary reaction mechanism is apparently inconsistent with our observations (Table 1), because Hg(II) is only weakly complexed with the LMWOCs used in the present study. Using Visual Minteq and a conservative stability constant of 10$^{16.7}$ (Visual Minteq database; Ravichandran, 2004) for the Hg-carboxylate complexes, we estimated that >88% of the Hg(II) was in the form of HgCl$_2$ in the reactant solution containing these organics. Indirect photo-oxidation thus is prevalent in the presence of non-thiol LMWOCs. Our results are consistent with those of Zheng and Hintelmann (2010), who reported that nuclear field shift effects dominated in the early stage of the photoreduction of Hg(II) in the presence of serine. Secondary reactions by radicals such as CO$_2^-$ and •COOH generated from the carboxyl group of serine were thus proposed by these authors as the dominant reaction mechanism for the reduction of Hg(II).
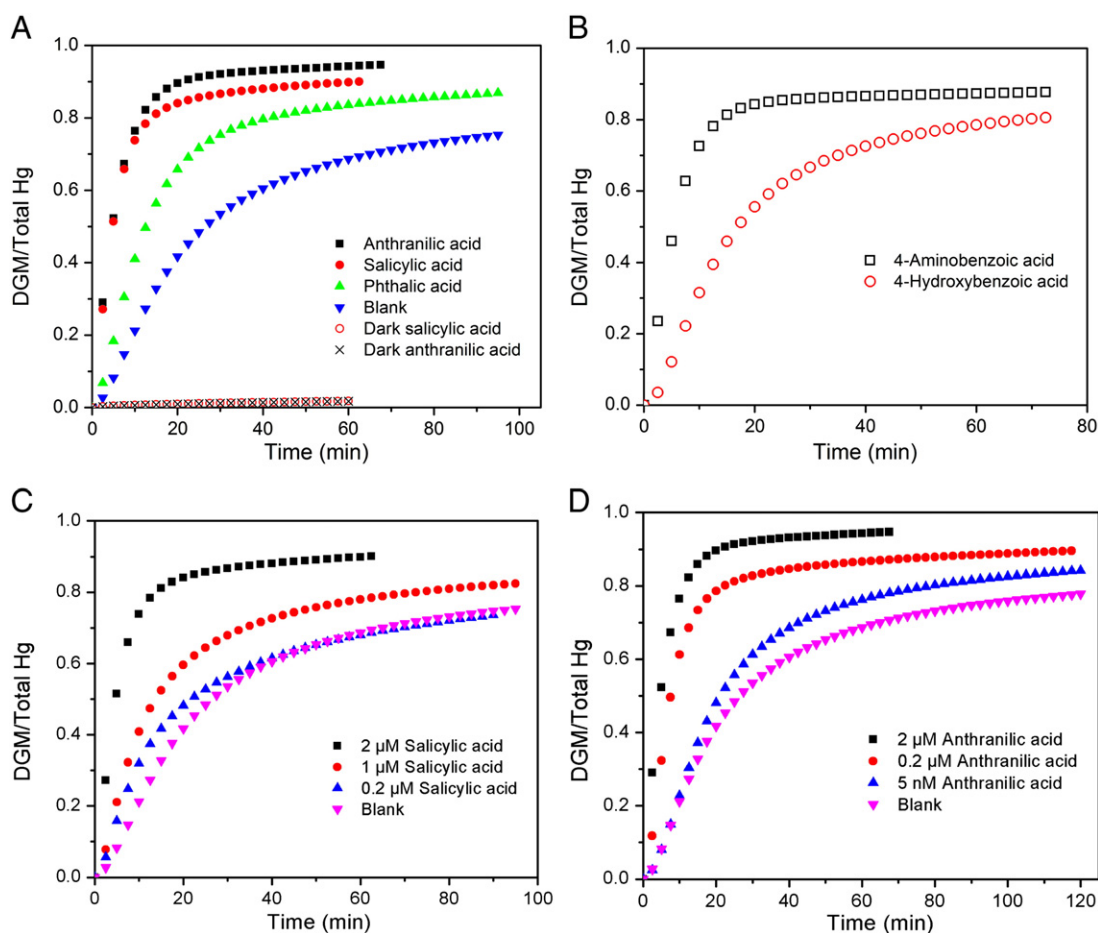
Fig. 1. Cumulative DGM production during Hg(II) photoreduction under UV-B irradiation. (a) effects of anthranilic, salicylic, phthalic acids (2 μM organic acids), no organics (blank), and dark controls (2 μM organic acids); (b) effects of 4-aminobenzoic and 4-hydrobenzoic acids (2 μM organic acids); (c) effects of salicylic acid concentration; (d) effects of anthranilic acid concentration. Experiments were performed at 1 nM Hg(II), pH 4.2 ± 0.3, and 60 μM Cl⁻. Estimated experimental errors between duplicate measurements were ± 10%.

3.2. Spectral absorption of LMWOCs and mechanisms of Hg(II) photoreduction

The photoreactivity of these LMWOCs and their corresponding free radicals produced are likely responsible for the observed differences in photoreduction rates of Hg(II). This hypothesis was tested by measuring the UV absorption of these organics (Fig. 2) and analyzing their absorption spectra with respect to the Hg(II) photoreduction rates (Table 1). Aromatic compounds often show strong absorption bands in the UV region due to the π–π* transition induced by π electrons on the benzene ring (Turro, 1978). For benzoic acid, the non-bonding electrons on C=O give rise to the n–π* transition, resulting in an absorption band that is centered at 269 nm (Supplementary Data Fig. S3). Introducing a substituent (i.e.,–COOH, –OH, or –NH₂) at the ortho position of benzoic acid red-shifts the absorption band from 269 nm (benzoic acid) to 280 nm (phthalic acid), 296 nm (salicylic acid), or 313 nm (anthranilic acid), respectively (Fig. 2). This red-shift in UV absorption indicates that a lower energy is required for electronic excitation of the organic molecules and is consistent with the energy required to produce an excited state at the n–π* transition. Using the absorption wavelength in the equation $E = h\nu$, we calculated this excitation energy to be 7.1×10^{-19}, 6.7×10^{-19}, 6.4×10^{-19} J, for phthalic, salicylic, and anthranilic acids, respectively (Turro, 1978). Under UV-B irradiation, both anthranilic and salicylic acids are photoreactive since their UV absorption peaks are centered at 313 and 296 nm. It is thus not surprising that they are the most reactive in reducing Hg(II) among all LMWOCs used in this study.

The photoreactivity of these organics also offers an explanation why the substitution of –OH on benzoic acid from the ortho- to para-position substantially decreased the photoreduction rates of Hg(II) (from 8.4 to 2.4 h⁻¹). With the ortho to para substitution, the absorption peak induced by the n–π* transition is blue-shifted from 296 nm (salicylic acid) to 250 nm (4-hydroxybenzoic acid), resulting in little or no UV-B absorption. However, in the case of aminobenzoic acid, although substitution of –NH₂ from the ortho- to
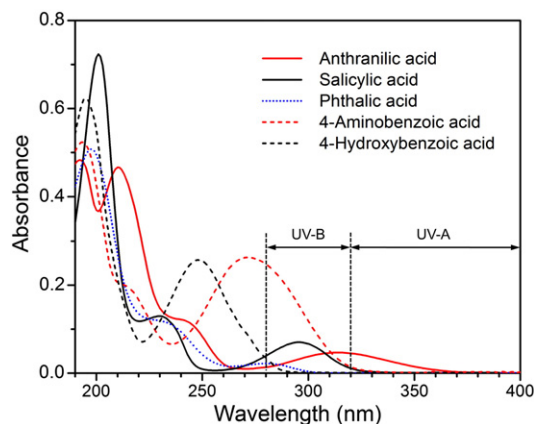

Fig. 2. UV absorption spectra of LMWOCs used in the present study. They were dissolved in DI water at 20 μM.

para-position also blue-shifts the absorption peak from 313 nm (anthranilic acid) to 271 nm (4-aminobenzoic acid), it still permits a substantial UV-B absorption (Fig. 2). As a result, only a moderate decrease in Hg(II) photoreduction rate was observed, from 8.8 (anthranilic acid) to 7.6 h^{-1} (4-aminobenzoic acid).

The correlations between photoreactivity of LMWOCs and their effects on Hg(II) photoreduction are further shown by comparative studies of the Hg(II) reduction rates under UV-A (320–400 nm) irradiation (Fig. 3). By shifting the irradiation from dominant UV-B to UV-A, the Hg(II) photoreduction rate did not change appreciably in the presence of anthranilic acid because the absorption band of this organic is centered at about 313 nm. However, under UV-A irradiation the Hg(II) photoreduction rates by 4-hydroxybenzoic acid, salicylic acid, and 4-aminobenzoic acid all decreased by nearly an order of magnitude compared with those obtained under UV-B irradiation (Table 1). This decrease is attributed to little or no UV-A absorption by these organic compounds. The UV-A absorption of these compounds follows the decreasing order anthranilic acid > 4-aminobenzoic acid > salicylic acid > 4-hydroxybenzoic acid (Fig. 2), which is the same as the order of their corresponding Hg(II) photoreduction rates (Table 1). We note that strong UV-A absorption by anthranilic acid likely contributed to relatively high photoreduction rates of Hg(II) observed under UV-B irradiation (with anthranilic acid) since UV-B lamps have 24.5% of irradiation energy in UV-A region.

The photoreduction of Hg(II) (as HgCl$_2$) was studied previously and thought to follow a ligand-to-metal charge transfer mechanism, which produces Hg(I) and Cl$^{\bullet}$ free radicals (Horvath and Vogler, 1993). Hg(I) can then undergo a disproportionation process to form Hg(0) and Hg(II) (Horvath and Miko, 1999). However, in the presence of photosensitive organics such as anthranilic and salicylic acids, which generally have greater photoabsorption than HgCl$_2$ (at ~240 nm) in the UV-B or UV-A range (Horvath and Vogler, 1993), the photolysis of these organic compounds may produce significant amounts of reactive radicals to drive Hg(II) photoreduction. In a study of the photolysis of anthranilic acid using a nanosecond flash laser, Pozdnyakov et al. (2009b) showed that the excitation of anthranilate anion (ABA^{-}) produced ABA^{-} triplet states, carboxyanilinyl radicals (ABA$^{\bullet}$), and e$_{aq}^{-}$. All three species can decay through recombination or by reacting with oxidants such as dissolved oxygen and Hg(II) in solution. Under oxidizing conditions, e$_{aq}^{-}$ and the triplet state were found to decay rapidly with lifetimes < 50 and ~160 ns, respectively (Pozdnyakov et al., 2009b). However, ABA$^{\bullet}$ shows a much longer lifetime and reaches a steady concentration at 50 μs post-excitation, suggesting that ABA$^{\bullet}$ radicals are the more likely reactive species than the triplet state and e$_{aq}^{-}$ in the

photoreduction of Hg(II). This conclusion is consistent with an early study, indicating that e$_{aq}^{-}$ is not a dominant reductant for Hg(II) photoreduction (O'Driscoll et al., 2004). Using an average steady-state concentration of 2×10^{-7} mol L^{-1} for e$_{aq}^{-}$ (adopted from Zepp et al. (1987)), O'Driscoll et al. (2004) showed that DGM produced from reduction of Hg(II) by e$_{aq}^{-}$ is 10,000 times lower than the observed DGM concentration in their study.

Similarly, the photolysis studies of salicylic acid and its derivative, sulfosalicylic acid (SSA), showed the production of corresponding triplet states, organic free radicals, and e$_{aq}^{-}$ (Pozdnyakov et al., 2004, 2006, 2007; Zhu et al., 2010). Pozdnyakov et al. (2006) showed that the formation of SSA$^{\bullet}$ radicals and its recombination lead to the formation of 3-(2-carboxy-4-sulfophenoxy)-sulfosalicylate. We can therefore infer that the formation of the carboxyanilinyl ABA$^{\bullet}$ and carboxyphenoxyl free radicals, pertinent to anthranilic acid and salicylate, is the primary cause for the photoreduction of Hg(II) during the photolysis of these organics as shown in Schemes 1 and 2.

The difference observed in the photoreduction rates of Hg(II) by anthranilic, salicylic acid, and others can be explained by both the production rate and reactivity of the organic free radicals produced during photolysis of these compounds. The quantum yield of e$_{aq}^{-}$ during photolysis of anthranilic acid was reported to be about five times higher than that of salicylic acid (Pozdnyakov et al., 2007, 2009a), due to the lower ionization potentials of aromatic amines than those of phenols (Line, 1996). Because the reactive radicals and e$_{aq}^{-}$ are generated at the same time during photoionization of the singlet state (Pozdnyakov et al., 2009b), a higher formation rate of radicals is expected for anthranilic acid than salicylic acid.

Previous studies on the reaction rates between oxygen and anilinyl- or phenoxyl-type radicals also suggest that anilinyl radical is more reactive than phenoxyl radical (Pozdnyakov et al., 2007, 2009b). The rates were found to be about an order of magnitude higher in the presence of anthranilic acid ($k_{O2} \approx 5 \times 10^7$ M^{-1}s^{-1}) (Pozdnyakov et al., 2009b) than salicylic acid ($k_{O2} \approx 2 \times 10^6$ M^{-1}s^{-1}) (Pozdnyakov et al., 2007). The reactivity of anilinyl and phenoxyl radicals toward oxygen was also demonstrated in our photolysis experiments without adding Hg(II) (Supplementary Data Fig. S4). By altering the purging gas from N$_2$ to air, we were able to compare the UV–vis spectral changes of the LMWOCs (~20 μM) during photolysis under UV-B irradiation. We found that, in the absence of oxygen, all organics showed negligible spectral changes, indicating that either the recombination or self-quenching of reactive free radicals or intermediates dominated the photolysis process. In the presence of oxygen, however, these compounds showed a significant decrease in both the UV peak intensity and the corresponding shift of peak positions, indicating degradation and transformation of salicylic and anthranilic acids as a result of reaction between oxygen and carboxyphenoxyl and ABA$^{\bullet}$ radicals. The degree of intensity changes of the UV–vis spectra (Supplementary Data Fig. S4) also qualitatively show that anilinyl- and phenoxyl-type radicals are more reactive than carboxyl radicals, and the ortho-substituted isomers are more reactive than the para-substituted isomers with respect to oxygen, consistent with the photoreduction rates of Hg(II) observed under similar conditions (Fig. 1 and Table 1).

4. Conclusions

This study demonstrates the importance of specific functional groups and their steric arrangements on LMWOCs in the photochemical
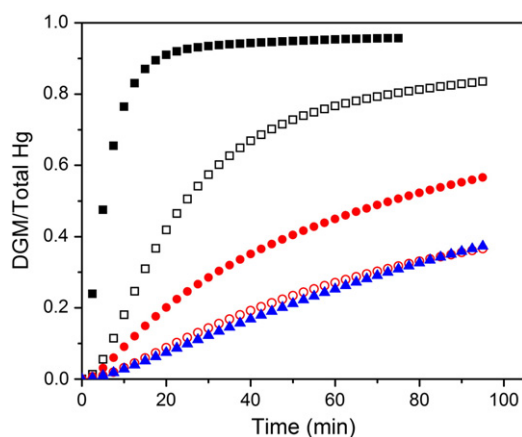

Fig. 3. Cumulative DGM production during photoreduction of Hg(II) in the absence (▲) or presence of anthranilic acid (■), 4-aminobenzoic acid (□), salicylic acid (●) and 4-hydroxybenzoic acid (○) under UV-A irradiation. The experiments were performed at pH 4.2 ± 0.3, 60 μM Cl^{-}, and 23 ± 1 °C. The initial Hg(II) concentration was 1 nM, organic concentration was 2 μM, and the UV-A irradiance intensity was 33.6 W m^{-2}.
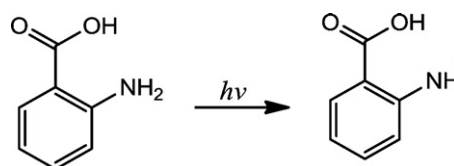
Scheme 1. Photolysis of anthranilic acid produces carboxyanilinyl radical.
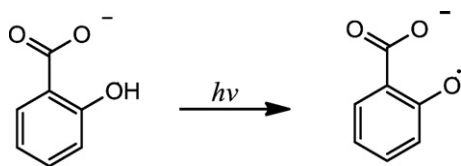
Scheme 2. Photolysis of salicylic acid produces carboxyphenoxyl radical.

transformation of Hg(II) in water. The photoabsorption characteristics of organics are closely correlated to the generation of organic free radicals and thus the photoreduction of Hg(II) through an indirect electron transfer mechanism. Our results could be useful for improved understanding of the photochemical redox transformation of Hg in both natural and contaminated environments. For example, Garcia et al. (2005) reported that UV-A tends to have an increased effect on photoreduction of Hg(II) in humic lakes and UV-B in clear lakes. They attributed these observations to differences of UV-A and UV-B in penetrating into waters with varying DOC concentrations (i.e., UV-A can penetrate deeper in water than UV-B). Our results suggest that stronger UV-A absorption by more humified organics also may have contributed to greater rates of photolysis of these organic materials and consequently more free radicals leading to the reduction of Hg(II).

The present study was performed under relatively low pH (4.2) and in the absence of dissolved oxygen conditions. Separate experiments were also performed at relatively high pH (~8) conditions, in which the observed pseudo-first-order rate constants for Hg(II) photoreduction by anthranilic and salicylic acids were about 8.0 and 8.2 h^{-1}, respectively, comparable with those observed at pH 4.2 (Supplementary Data Fig. S5). These observations suggest that the secondary reaction or generation of organic radicals in the presence of LMWOCs, as described earlier for pH 4.2 experiments, still dominates in the system, despite changes of the Hg(II) speciation and the deprotonation of carboxyl groups in anthranilic acid at pH 8 (Table 1). In this case, Hg(II) is present primarily as Hg(OH)$_2$ at pH 8.0 as opposed to HgCl$_2$ at pH ~4.2 (Dong et al., 2010). However, the fact that both UV-B and UV-A absorbance spectra of these organics did not change appreciably (Fig. S6) supports above conclusions. We extend these observations to the environments, where relatively low pH (4.2) conditions have been observed in contaminated environments such as acid lakes (Brown et al., 2010) and atmospheric waters or acidic fog with very low pH (i.e., pH 2–5) (Lin and Pehkonen, 1997; Si and Ariya, 2008). We expect that Hg(II) photoreduction by these organic compounds proceeds with similar rates in pH range of 4–8 since the absorbance spectra of the LMWOCs are not changing in this pH range. Additional studies in the presence or absence of other naturally occurring redox species and thiol compounds are underway in order to fully elucidate the mechanisms of Hg(II) photoreduction in the natural ecosystem. These studies are expected to further contribute to the understanding of the role of natural organics in Hg photoredox transformation and geochemical cycling.

Acknowledgement

Appendix A. Supplementary Data

Supplementary data to this article can be found online at doi:10.1016/j.scitotenv.2011.11.081.

References

Ababneh FA, Scott SL, Al-Reasi HA, Lean DRS. Photochemical reduction and reoxidation of aqueous mercuric chloride in the presence of ferrioxalate and air. Sci Total Environ 2006;367:831–9.
Amyot M, Mierle G, Lean DRS, Mcqueen DJ. Sunlight-induced formation of dissolved gaseous mercury in lake waters. Environ Sci Technol 1994;28:2366–71.
Amyot M, Gill GA, Morel FMM. Production and loss of dissolved gaseous mercury in coastal seawater. Environ Sci Technol 1997a;31:3606–11.
Amyot M, Mierle G, Lean D, McQueen DJ. Effect of solar radiation on the formation of dissolved gaseous mercury in temperate lakes. Geochim Cosmochim Acta 1997b;61:975–87.
Benner R, Pakulski JD, McCarthy M, Hedges JI, Hatcher PG. Bulk chemical characteristics of dissolved organic-matter in the ocean. Science 1992;255:1561–4.
Bonzongo J, Donkor AK. Increasing UV-B radiation at the earth's surface and potential effects on aqueous mercury cycling and toxicity. Chemosphere 2003;52:1263–73.
Brinkmann T, Horsch P, Sartorius D, Frimmel FH. Photoformation of low-molecular-weight organic acids from brown water dissolved organic matter. Environ Sci Technol 2003;37:4190–8.
Brown D, Goncharov A, Paul E, Simonin H, Carpenter DO. The relationship between Adirondack Lake pH and levels of mercury in Yellow Perch. J Aquat Anim Health 2010;22:280–90.
Dong W, Liang L, Brooks S, Southworth G, Gu B. Role of dissolved organic matter in the speciation of mercury and methylmercury in a contaminated ecosystem in Oak Ridge, Tennessee. Environ Chem 2010;7:94-102.
Dong W, Bian Y, Liang L, Gu B. Binding constants of mercury and dissolved organic matter determined by a modified ion exchange technique. Environ Sci Technol 2011;45:3576–83.
Garcia E, Amyot M, Ariya P. Relationship between DOC photochemistry and mercury redox transformations in temperate lakes and wetlands. Geochim Cosmochim Acta 2005;69:1917–24.
Gu B, Bian Y, Miller CL, Dong W, Jiang X, Liang L. Mercury reduction and complexation by natural organic matter in anoxic environments. Proc Natl Acad Sci U S A 2011;108:1479–83.
Haitzer M, Aiken GR, Ryan JN. Binding of mercury(II) to dissolved organic matter: The role of the mercury-to-DOM concentration ratio. Environ Sci Technol 2002;36:3564–70.
Horvath O, Miko I. Intermediates in photoinduced reactions of Hg-2(2+) in aqueous solution. Inorg Chem Commun 1999;2:143–5.
Horvath O, Vogler A. Photoredox chemistry of chloromercurate(Ii) complexes in acetonitrile. Inorg Chem 1993;32:5485–9.
Krabbenhoft DP, Hurley JP, Olson ML, Cleckner LB. Diel variability of mercury phase and species distributions in the Florida Everglades. Biogeochemistry 1998;40:311–25.
Lin CJ, Pehkonen SO. Aqueous free radical chemistry of mercury in the presence of iron oxides and ambient aerosol. Atmos Environ 1997;31:4125–37.
Line D. Handbook of Chemistry and Physics. Roca Raton: CRC Press; 1996.
Moran MA, Zepp RG. Role of photoreactions in the formation of biologically labile compounds from dissolved organic matter. Limnol Oceanogr 1997;42:1307–16.
O'Driscoll NJ, Beauchamp S, Siciliano SD, Rencz AN, Lean DRS. Continuous analysis of dissolved gaseous mercury (DGM) and mercury flux in two freshwater lakes in Kejimkujik Park, Nova Scotia: evaluating mercury flux models with quantitative data. Environ Sci Technol 2003;37:2226–35.
O'Driscoll NJ, Lean DRS, Loseto LL, Carignan R, Siciliano SD. Effect of dissolved organic carbon on the photoproduction of dissolved gaseous mercury in lakes: potential impacts of forestry. Environ Sci Technol 2004;38:2664–72.
O'Driscoll NJ, Siciliano SD, Lean DRS, Amyot M. Gross photoreduction kinetics of mercury in temperate freshwater lakes and rivers: application to a general model of DGM dynamics. Environ Sci Technol 2006;40:837–43.
Poulain AJ, Amyot M, Findlay D, Telor S, Barkay T, Hintelmann H. Biological and photochemical production of dissolved gaseous mercury in a boreal lake. Limnol Oceanogr 2004;49:2265–75.
Pozdnyakov IP, Plyusnin VF, Grivin VP, Vorobyev DY, Kruppa AI, Lemmetyinen H. Photochemistry of sulfosalicylic acid in aqueous solutions. J Photochem Photobiol A 2004;162:153–62.
Pozdnyakov IP, Plyusnin VF, Grivin VP, Vorobyev DY, Bazhin NM, Vauthey E. Photolysis of sulfosalicylic acid in aqueous solutions over a wide pH range. J Photochem Photobiol A 2006;181:37–43.
Pozdnyakov IP, Sosedova YA, Plyusnin VF, Grivin VP, Bazhin NM. Photochemistry of salicylate anion in aqueous solution. Russ Chem B 2007;56:1318–24.
Pozdnyakov IP, Pigliucci A, Tkachenko N, Plyusnin VF, Vauthey E, Lemmetyinen H. The photophysics of salicylic acid derivatives in aqueous solution. J Phys Org Chem 2009a;22:449–54.
Pozdnyakov IP, Plyusnin VF, Grivin VP. Photophysics and photochemistry of 2-aminobenzoic acid anion in aqueous solution. J Phys Chem A 2009b;113:14109–14.
Qureshi A, O'Driscoll NJ, MacLeod M, Neuhold YM, Hungerbuhler K. Photoreactions of mercury in surface ocean water: gross reaction kinetics and possible pathways. Environ Sci Technol 2010;44:644–9.
Ravichandran M. Interactions between mercury and dissolved organic matter — a review. Chemosphere 2004;55:319–31.
Si L, Ariya PA. Reduction of oxidized mercury species by dicarboxylic acids (C-2-C-4): kinetic and product studies. Environ Sci Technol 2008;42:5150–5.
Sillen LG, Martell AE, Bjerrum J. Stability Constants of Metal-Ion Complexes. London: Chemical Society; 1964.
Turro NJ. Modern molecular photochemistry. Merlo Park: The enjamin/cummings publishing company; 1978.
Xiao ZF, Stromberg D, Lindqvist O. Influence of humic substances on photolysis of divalent mercury in aqueous-solution. Water Air Soil Pollut 1995;80:789–98.

Zepp RG, Braun AM, Hoigne J, Leenheer JA. Photoproduction of hydrated electrons from natural organic solutes in aquatic environments. Environ Sci Technol 1987;21: 485–90.

Zhang H. Photochemical redox reactions of mercury. Recent Dev Mercury Sci 2006;120:37–79.

Zhang H, Dill C. Apparent rates of production and loss of dissolved gaseous mercury (DGM) in a southern reservoir lake (Tennessee, USA). Sci Total Environ 2008;392:233–41.

Zhang H, Lindberg SE. Sunlight and iron(III)-induced photochemical production of dissolved gaseous mercury in freshwater. Environ Sci Technol 2001;35:928–35.

Zheng W, Hintelmann H. Mercury isotope fractionation during photoreduction in natural water is controlled by its Hg/DOC ratio. Geochim Cosmochim Acta 2009;73:6704–15.

Zheng W, Hintelmann H. Isotope fractionation of mercury during its photochemical reduction by low-molecular-weight organic compounds. J Phys Chem A 2010;114:4246–53.

Zheng W, Liang L, Gu B. Mercury reduction and oxidation by reduced natural organic matter in anoxic environments. Environ Sci Technol in press.

Zhou XL, Mopper K. Photochemical production of low-molecular-weight carbonyl compounds in seawater and surface microlayer and their air-sea exchange. Mar Chem 1997;56:201–13.

Zhu H, Wang M, Cheng LL, Zhu RR, Sun XY, Yao SD, et al. Photoionization and photoexcitation mechanisms of salicylic acid. Acta Phys-Chim Sin 2010;26:87–93.